PRIFYSGOL

# glyndŵr
UNIVERSITY

**Glyndŵr University Research Online**

**Conference Paper**

# Performance comparison between copper and aluminium windings in a rim driven fan for a small unmanned aircraft application

Bolam, R.C., Vagapov. Y. and Anuchin, A.

**Recommended citation:**

Bolam, R.C., Vagapov. Y. and Anuchin, A. (2020), 'Performance comparison between copper and aluminium windings in a rim driven fan for a small unmanned aircraft application'. In: Proc. 11th Int. Conf. on Electrical Power Drive Systems (ICEPDS), Saint-Petersburg, Russia, 4-7 Oct. 2020, pp. 1-6. doi: 10.1109/ICEPDS47235.2020.9249076

# Performance Comparison between Copper and Aluminium Windings in a Rim Driven Fan for a Small Unmanned Aircraft Application

Robert Cameron Bolam
*Glyndwr University*
Wrexham, UK

Yuriy Vagapov
*Glyndwr University*
Wrexham, UK

Alecksey Anuchin
*Moscow Power Engineering Institute*
Moscow, Russia

*Abstract*—**Rim Driven Fans (RDFs) are receiving increased attention amongst zero-emission aerospace technologists as they offer the potential for high Fan Pressure Ratios (FPR) to be efficiently generated and fan flow to be maximised compared with conventional (hub driven) electrical axial-flow fans. In other words; RDFs can provide higher thrust performance and exhaust air velocities than hub driven devices of the same intake area and also offer significant aerodynamic drag reductions. As such they are a feasible propulsion contender for fixed-wing, distributed-thrust, electrical aircraft designs. Thrust-to-weight ratio is a critical design parameter when considering aircraft propulsion devices and so design mass must be optimised accordingly. This paper presents an electromagnetic comparison of copper versus aluminium, slot-less, brushless DC motor (BLDC), stator-wiring architectures. The results of this study identify the performance benefits and limitations of these differing stator wiring materials in the context of a single rotor-stage RDF intended for the propulsion of a small unmanned aircraft.**

*Keywords*—*rim driven fan, RDF, unmanned aircraft, electric aircraft, aluminium windings, ironless rotor, specific power*

## I. INTRODUCTION

Electrical rim drive technology has been around for decades and is particularly popular for marine propulsion devices such as Rim Driven Thrusters [1]. One obvious benefit of a rim drive is that greater leverage is achieved from a tangential force applied at the rim of a rotor than one applied at or near its hub. Other benefits include less obstruction to the through-flow of fluids if used in an RDF or RDT application and the flexibility to install multiple rim driven devices in tandem. Some of the main disadvantages of rim drives are that they are: susceptible to efficiency reductions due to friction generated at the rim, for example from rim mounted mechanical bearings; they may require relatively high supply current frequencies to achieve fast rotational speeds and noise, vibration and harshness (NVH) problems can arise owing to the manifestation of eddy currents, cogging torque and torque-ripple effects at the rim [2]. Some motors are more suited to rim drives than others, with the better types being induction motors (IMs) and brushless DC (BLDC) motors. These motors have the benefits of being robust in design, require no electrical supply to the rotor and exhibit good power densities. This study compares copper with aluminium stator windings for a BLDC motor, in a rim driven fan

application, intended to propel a small unmanned aircraft. It is worth noting that aluminium conductors are already commonplace in components such as IMs, transformers [3]-[7] and National Grid power lines.

Thrust to weight ratio is a critical design parameter when considering aircraft propulsion mechanisms [8] and literature already exists whereby motors have been compared having aluminium and copper windings. In a study of aluminium versus copper stator windings for single-phase induction motors [9] two single-phase 0.25 kW, 230 VAC (max 3,000 RPM) motors were tested across their operational range with aluminium and copper wired stators. The main reason for this study was economic in nature (aluminium being lower in cost) and demonstrated that the performance of the two differently wound motors was "almost the same". This study also found reduced weight and noise levels with aluminium windings. In [10], a comparative study between aluminium and copper windings was conducted on a machine fitted with the alternate materials. The purpose is being to assess the feasibility of using aluminium for cost-effective in-volume motor fabrication. A variable-speed interior permanent magnet BLDC motor, for a traction application 60 kW, DC link voltage 600 V (0-15 kRPM with a base speed of 4,770 RPM), was studied. This study found that only a moderate reduction in machine performance is experienced with aluminium windings. Concluding that in this particular case for a small 2% reduction in efficiency over the vehicle driving cycle there would be an overall mass saving of 3kg.

In the study presented in this paper, the masses of the active components of the BLDC design have been minimised. The rotor iron deleted and the stator back-iron has been paired down to saturate at a flux density of 1.8 T. BLDC motors can be categorised by their permanent magnet (PM) installations which are surface mounted (SPM) or flux concentrating, interior (IPM) configurations. The surface-mounted type has been chosen for this study as it is more amenable to achieving thin rim designs. The permanent magnetic field is a Halbach array to maximise the air-gap flux density and a 1mm thick CFRP magnet retaining sleeve has been included in the analysis owing to the high operational speed of the rotor (> 20,000 RPM).

## II. RDF PERFORMANCE REQUIREMENT

The RDF's shaft power requirement was used to relate the electrical motor design to its fan performance over a range of rotational speeds from zero to 25,000 RPM. Initially, the fan pressure ratio (FPR) was calculated using (1), based on Euler's principle of angular momentum [11] and a whirl velocity difference $\Delta C_w = 0.017U$, which is a

representative value for small fan blade designs of this type.

$$FPR = \frac{P_{Tout}}{P_{Tin}} = \left(1 + \eta_s \frac{U \Delta C_w}{C_p T_o}\right)^{\frac{\gamma}{(\gamma-1)}} \qquad (1)$$

where $P_{Tout}$ is fan outlet pressure (total), Pa; $P_{Tin}$ is fan inlet pressure (total), Pa; $C_p$ is specific heat capacity (of air) at constant pressure (taken as 1005 J/kg·K); $T_o$ is static air temperature, K; $\gamma$ is ratio of specific heat capacities ($C_p/C_v$) for air ($\gamma = 1.4$); $\eta_s$ is isentropic efficiency (fan), %.

The *FPR* was calculated for the range of RDF speeds and the differential pressure generated across the fan rotor was established with (2).

$$\Delta p = \left(FPR \times p_o\right) - p_o \qquad (2)$$

where $\Delta p$ is difference in pressure, Pa; $p_o$ is static pressure, Pa.

The RDF volumetric *V* and mass *M* airflow were calculated with equations (3) and (4).

$$\dot{V} = K\sqrt{\frac{2\Delta p}{\rho}} \times \pi \left(r_{rim}^2 - r_{hub}^2\right) \qquad (3)$$

$$\dot{M} = \dot{V}\rho \qquad (4)$$

where *K* is a dimensionless fan flow parameter taken as 0.95; $\rho$ is air density, kg/m³; $r_{rim}$ is rim radius, m; $r_{hub}$ is hub radius, m.

The RDF shaft (motor output) power *P*, torque *T* and *Thrust* were determined using (5)-(7).

$$P = \dot{M}U\Delta C_w \qquad (5)$$

$$T = \frac{P}{\omega} \qquad (6)$$

$$Thrust = \dot{M} \times \Delta v \qquad (7)$$

where $\omega$ is angular velocity, rad/s; $\Delta v$ is difference in velocity, m/s.

Table I details the results of the above calculations and Fig. 1 shows the desired RDF fan performance curves over a range of rotational speeds from zero to 25,000 RPM. Fig. 1(a) represents the RDF's aerodynamic start-up performance, showing the pressure rise and flowrate increasing as a result of the fan's acceleration. Fig. 1(b) is the RDF's torque versus speed characteristic and represents the output power (shaft power) required of the RDF's motor. Fig. 1(c) is the RDF's thrust versus speed characteristic and indicates the static-thrust attainable for a given speed.
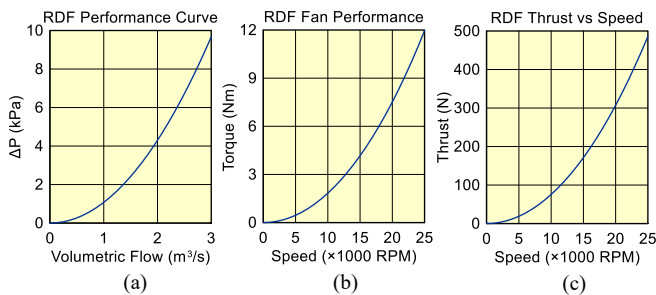


Fig. 1. Desired RDF fan performance characteristics.

TABLE I.   RDF MOTOR AND FAN AERODYNAMIC PERFORMANCE PARAMETERS.

| RDF Speed (RPM) | 0 | 5,000 | 10,000 | 15,000 | 20,000 | 25,000 |
|---|---|---|---|---|---|---|
| **Shaft Power (W)** | 0 | 279.9 | 2244.2 | 7600.4 | 18103.1 | 34108.5 |
| **Shaft Torque (Nm)** | 0 | 0.535 | 2.143 | 4.839 | 8.644 | 13.028 |
| **RDF Pressure Rise (ΔP) (Pa)** | 0 | 393.7 | 1581.4 | 3582.9 | 6431.4 | 10174.5 |
| **RDF Volumetric Flow (m³/s)** | 0 | 0.605 | 1.213 | 1.826 | 2.447 | 3.077 |
| **RDF Massflow (kg/s)** | 0 | 0.742 | 1.486 | 2.237 | 2.997 | 3.614 |
| **RDF Static Thrust (N)** | 0 | 18.8 | 75.5 | 171.1 | 307.1 | 465.8 |

III.   ALUMINIUM VERSUS COPPER WINDINGS

The two most common materials, used by the wire and cable industry to conduct electricity are copper and aluminium. The International Annealed Copper Standard (IACS) allows a comparison to be made, between copper and other metals, with copper rated at 100% conductivity. Aluminium has 61% of the conductivity of copper but at 30% of its weight. Table II provides a comparison between copper and aluminium for the same domestic wiring application [12]. It was determined that aluminium conductors typically had to be two AWG sizes larger than copper conductors for the same application.

The vast majority of electrical motors have been designed for terrestrial or marine applications and employ copper windings. However, the RDF is an aerospace application. Therefore, a performance comparison, between an otherwise identical RDF device was conducted to investigate whether there was a potential to optimise its weight using aluminium instead of copper windings.

IV.   SPECIFIC POWER (POWER-TO-WEIGHT RATIO)

Specific power is an ideal parameter for the initial assessment of the performance of an aerospace propulsive device such as the RDF. Table III provides an approximate comparison of Specific Power values for traditional forms of vehicle engines

Specific Power values for high performance electrical motors usually lie between those of reciprocating and jet engines. In the study detailed in this paper the RDF specific power calculations have been based on the active masses of the motors.

TABLE II.   COMPARISON BETWEEN COPPER AND ALUMINIUM FOR THE SAME DOMESTIC WIRING APPLICATION.

| Properties | Copper | Aluminium |
|---|---|---|
| AWG size for 60 A @ 75ºC | 8 | 6 |
| Weight per 1,000 ft | 65 lb | 39 lb |
| Nominal diameter | 0.23 in. | 0.26 in. |
| Maximum pulling tension | 132 lb | 157 lb |

TABLE III. AN APPROXIMATE COMPARISON OF SPECIFIC POWER VALUES FOR TRADITIONAL FORMS OF VEHICLE ENGINES.

| Engine Type | Specific Power (kW/kg) |
|---|---|
| Automobile Engine (reciprocating) | 0.9 |
| High Performance Car Engine (reciprocating) | 4.8 |
| Jet Engine | 31 |
| Rocket Engine | 153 |

## V. RDF Motor Design

The rim drive motor models being compared, RDF-Al and RDF-Cu, have been designed with a four pole-pair surface-mounted permanent magnet rotor secured with 1mm thick banding. To minimise the RDF weight and rotating loads the rotor-iron has been omitted. The clearance (air gap) between the rotor magnets and stators is 2 mm and the permanent magnets are the rare-earth type made from neodymium iron boron (NeFeB) grade N42UH. The RDF is a slotless BLDC design and the stator is made from laminated electric steel grade M250-35A for which the thickness has been optimised to operate below the material flux saturation threshold of 1.8 Tesla. The double layer winding patterns are of insulated aluminium wire for RDF-Al, and insulated pure copper wire for RDF-Cu. Fig. 2 shows the slotless motor with the windings effectively sitting within an extended motor air-gap. The 3-phase windings comprise of four coils per phase each coil having 20 turns (40 conductor lengths) of AWG 13 (1.9025 -1.8288 mm, diameter) wire.
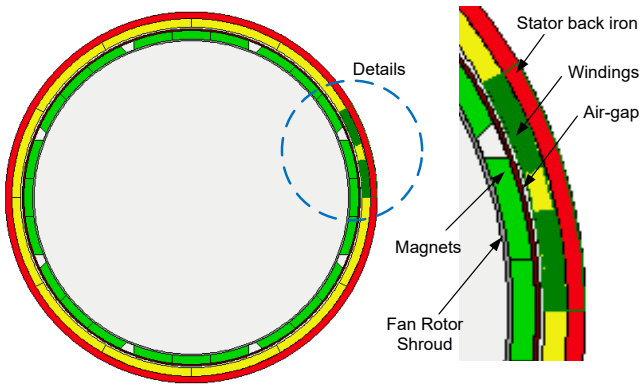


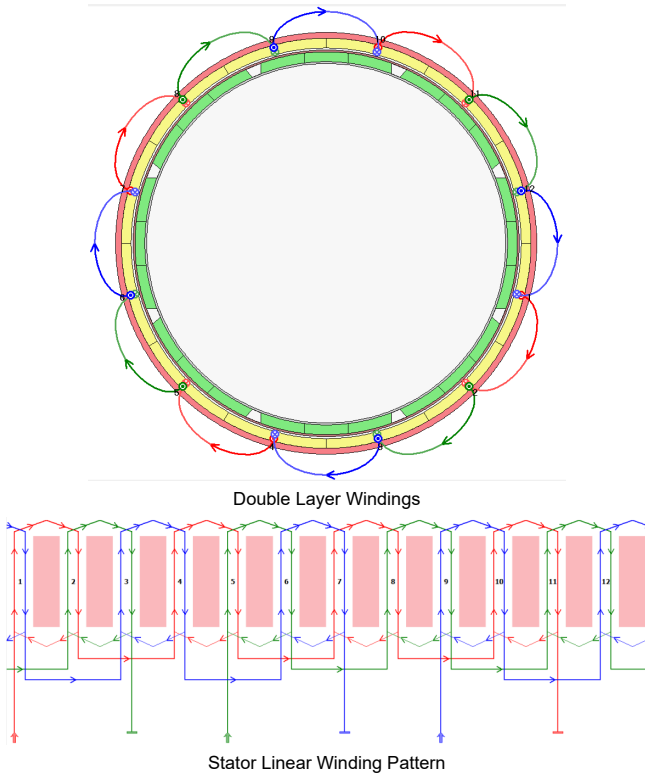Fig. 2. RDF rotor and stator arrangement and detail view of rim drive.



Fig. 3. Double layer windings and stator linear winding pattern.

TABLE IV. RDF DESIGN SPECIFICATION.

| Peak Torque | 8.6 Nm |
|---|---|
| Peak Power | 18.1 kW |
| Maximum Speed | 20000 RPM |
| DC Link Voltage | 370 V |
| Maximum current | 50 A (peak) |
| Stator Outer Diameter | 216 mm |
| Cooling | Forced Air Convection |
| Maximum temperature | 60°C |
| Air gap length | 2 mm |

The RDF motor's design specification is given in Table IV.

A three-phase, star connected, double layer winding pattern was used for both the copper and aluminium RDF performance analyses, refer to Fig. 3.

The analysis is based on a 370 VDC electrically supplied inverter delivering a balanced sinusoidal 3-phase supply to the RDF windings having a peak current value of 50 A as shown in Fig. 4(a).

## VI. Analysis

The RDF motor winding comparison was conducted using Motor-CAD software provided by Motor Design Ltd. of the UK. Initially the Motor-CAD EMag design tool was used to define the motor architecture and the layout of the windings. Then the Motor-CAD Lab design tool was used. Which enabled rapid analysis of the electric machine design over the full operating envelope providing the torque, power and efficiency characteristics. The software achieved this using a combination of numerical 2D finite element analyses (FEA) and analytical algorithms [13-19]. The Motor-CAD FEA solver automatically handled meshing, boundary conditions and symmetry. A thermal analysis was not conducted as the comparison was made considering that adequate ram-air cooling was available to maintain the overall RDF and electromagnetic components at 60°C.
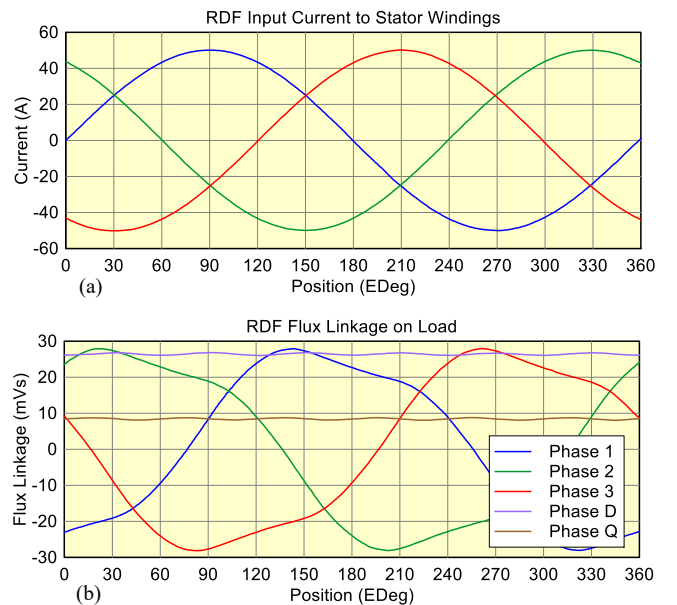


Fig. 4. (a) RDF input current to stator windings; (b) RDF flux linkage on load.

The electromagnetic modelling in Lab is based on the *d-q* axis model and assumes ideal sinusoidal flux linkages and current waveforms. Which allows an expression for both the steady-state electromagnetic torque and supply voltage to be derived:

The voltages in the *d-q* reference frame were derived using:

$$V_d = -\omega_s \psi_q + R I_d$$
$$V_q = -\omega_s \psi_d + R I_q \qquad (8)$$

where $\omega_s$ is the electrical supply angular frequency in rad/sec; $\psi_q$ and $\psi_d$ are the *d-q* axis flux linkages; $R$ is the circuit resistance.

By ignoring the resistive ($RI$) terms the stator voltage was derived using:

$$V_s = \omega_s \sqrt{\psi_d^2 + \psi_q^2} \qquad (9)$$

The average output power conversion over one electrical cycle was determined by:

$$P = \frac{m}{2}\left(V_d I_d + V_q I_q\right) = \frac{m}{2}\omega_s\left(\psi_d I_q - \psi_q I_d\right) \qquad (10)$$

where $P$ is the output (shaft) power; $m$ is the number of phases.

And the electromagnetic torque was calculated using:

$$T_e = \frac{P}{\omega} = \frac{3}{2}p\left(\psi_d I_q - \psi_q I_d\right) \qquad (11)$$

where $T_e$ is the RDF torque; $p$ is the number of pole-pairs.

Fig. 4(b) shows the on-load RDF flux linkages which were identical for both the copper and aluminium winding patterns.

### A. Flux Density Distributions

The flux density distributions in the stators and rotors of the copper and aluminium wound RDF models for peak torque operation is shown in Fig. 5. In both cases the flux densities can be seen to be identical with a maximum stator back-iron peak flux density of 1.72 Tesla. Which remains below the target magnetic saturation threshold of 1.8 Tesla.

### B. Electromagnetic Performance Results

The results of the Motor-CAD Lab analysis allowed the performance of the RDF motor, with copper and aluminium windings, to be plotted alongside the RDF fan torque-speed
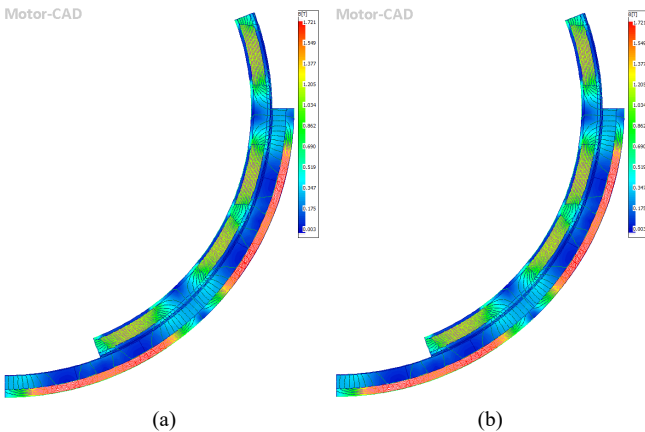
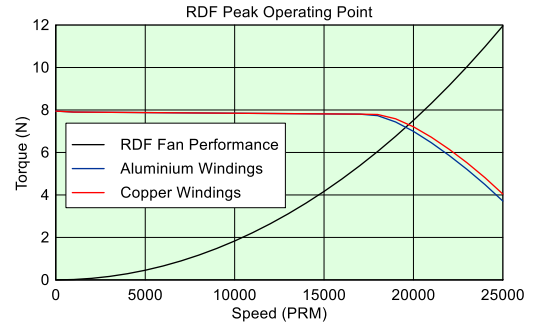Fig. 5. Flux distribution (a) copper and (b) aluminium windings.

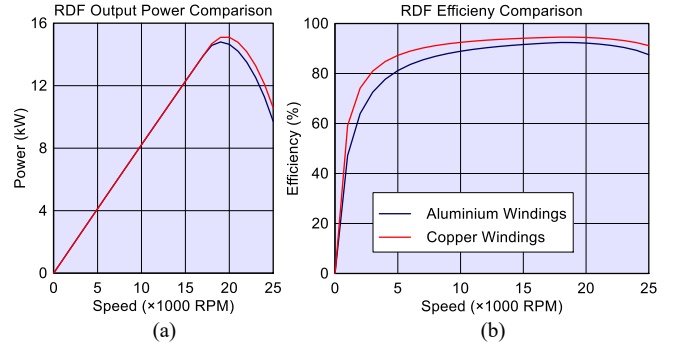Fig. 6. RDF torque versus speed for copper and aluminium windings.

Fig. 7. (a) RDF power versus speed and (b) RDF efficiency comparison for copper and aluminium windings.

characteristic. Fig. 6 shows the intersection of these two RDF motor curves, with the fan performance curve, occurring below 20 kRPM. The copper wound RDF demonstrated marginally better output torque (7.21 Nm) performance than the aluminium wound RDF (6.99 Nm) at 20 kRPM. The intersection points in both cases indicate the peak operating point for that particular RDF motor-fan combination and power supply conditions. The horizontal region of the RDF motor characteristics is identical for both RDF configurations and is an indication that the torque output is being limited by the available current (Mode I) and input voltage increases linearly with speed. The peak operating point (RDF Fan intersection) occurs beyond Mode I in the voltage and current limited region (Mode II) which results in a higher rotational speed for the same voltage however with a reduction in torque [20].

Fig. 7(a) provides a comparison of the RDF output power (shaft power) with copper and aluminium windings. These curves indicate the operating range of the RDF based on the limitation of the 370 VDC bus voltage. Again, it can be seen that the copper windings (15.1 kW @20 kRPM) provide only a marginal performance improvement over the RDF configured with aluminium windings (14.65 kW @20 kRPM).

An efficiency analysis was also conducted using the Motor-CAD Lab software and the results are shown in Fig. 7(b). Although both the copper and aluminium RDF configurations demonstrated very good efficiency characteristics over the entire operational speed range of the RDF. The copper wound stator exhibited the highest values with a peak efficiency at 20 kRPM of 94.4% compared with 92.2% for the aluminium wound stator

### C. Noise Vibration Harshness (NVH)

A slotless rotor design was selected for this analysis in order to minimise the RDF torque ripple and cogging torque effects which can severely impact the Noise
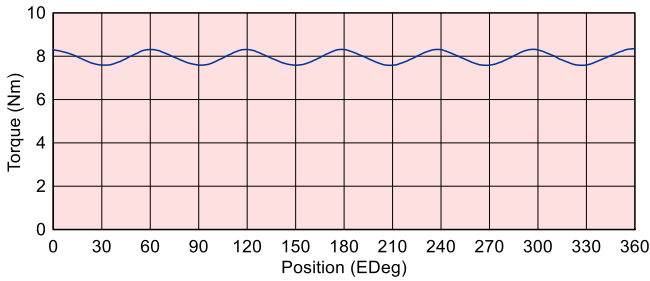
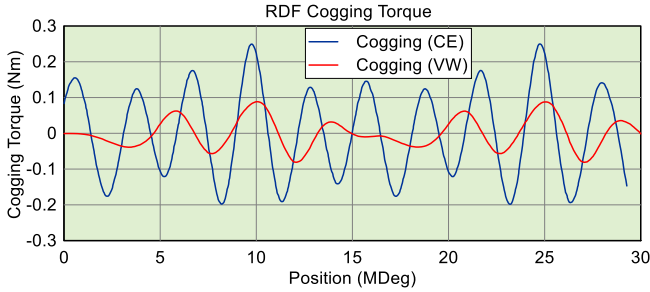Fig. 8. RDF continuous torque plot with ripple characteristic.



Fig. 9. RDF cogging torque plot.

| RDF Parameter | Copper (Cu) Windings | Aluminium (Al) Windings |
|---|---|---|
| Active Mass (kg) | 2.883 | 1.92 |
| Speed (RPM) | 20,000 | 20,000 |
| Output Power (kW) | 15.1 | 14.6 |
| RDF Torque (Nm) (@20kRPM) | 7.21 | 6.99 |
| Motor Efficiency (%) | 94.4 | 92.2 |
| Specific Power (kW/kg) (active elements) | 5.24 | 7.6 |

The Motor-CAD Lab software proved an excellent time-saving tool with which to conduct a quick trade-off study such as this. It was also interesting to note the high motor efficiencies obtained throughout the operational range of the RDFs. These were attributed in part to the slotless design and reduction in ferrous content of the RDF thus minimising eddy current (iron) losses and also for the aluminium windings which due to higher electrical resistivity is less prone to AC effects in this relatively high speed (supply frequency) BLDC application. The results of this study also concur with the findings and conclusions of the previously reviewed literature and in particular those of [9],[10].

It is planned for future work to include thermal analysis of a detail designed RDF with an aluminium stator and ram air cooling provision of the coils and associated electromagnetic elements.

Vibration and Harshness (NVH) properties of the rim driven device. Both the aluminium and copper windings demonstrated identical torque ripple and cogging torque effects as shown in Fig. 8 and Fig. 9 respectively. The cogging torque calculations were achieved using the magnetic co-energy variation method (CE) and also the virtual work (VW) computation method [13-19].

*D.   Comparison of Results*

Table V provides an overview of the RDF performance analysis results of the copper versus aluminium windings. The results indicate that copper provides a 3.3%, and 2.2% increase, in output (power/torque) and motor efficiency respectively, when compared with the aluminium windings. However, the aluminium windings provide a more significant 45% increase in specific power performance.

VII.   CONCLUSION

This analysis was conducted primarily to evaluate whether there may be performance advantages to be gained from using aluminium in place of copper windings in an aerospace application of a rim driven fan. And initial specific power results have confirmed that aluminium would make a preferable winding material providing a 45% increase in power to weight performance. It is worth noting that the specific power values have been calculated using the mass of the active elements of the circuitry and do not account for RDF structure and housing etc. Although, it can be considered that these non-active elements would be of equal masses for both the aluminium and copper RDF assemblies, their overall effect would be to reduce the percentage difference in power to weight ratio.

The performances of both of the RDF-Cu and RDF-Al models fell short of the initial design specification targets set out in Table 1 in regard to desired output power and torque. This would manifest itself in actual reduced RDF operating speeds and thrust generation. However, it was not the aim of this study to satisfy the exact specification values. This would entail further iterative modifications to the RDFs geometry and winding patterns.

REFERENCES

[1] Voith (2016). *The Reference in Silent Thrusters: Voith Rim Drive Technology in Yachts*. [Online]. Available: https://d2euiryrvxi8z1.cloudfront.net/asset/445934742530/b0fd56c0f731b4eb42fb9ba0b12d9a26

[2] R. Bolam, and Y. Vagapov, "Implementation of electrical rim driven fan technology to small unmanned aircraft," in *Proc. 7th IEEE Int. Conf. on Internet Technologies and Applications ITA-17*, Wrexham, UK, 12-15 Sept. 2017, pp. 35-40.

[3] C.R. Sullivan, "Aluminium windings and other strategies for high frequency magnetic design in an era of high copper and energy costs," *IEEE Trans. on Power Electronics*, vol. 23, no. 4, pp. 2044-2051, 2008.

[4] R. Wrobel, D. Salt, N. Simpson, and P. H. Mellor, "Comparative study of copper and aluminium conductors - Future cost effective PM machines," in *Proc. 7th IET Int. Conf. on Power Electronics, Machines and Drives (PEMD 2014)*, Manchester, UK, 8-10 April 2014, pp. 1-6.

[5] J. D. Widmer, R. Martin, and B.C. Mecrow, "Pre-compressed and stranded aluminium motor windings for traction motors," in *Proc. IEEE Int. Electric Machines and Drives Conf. (IEMDC)*, Coeur d'Alene, ID, USA, 10-13 May 2015, pp. 1851-1857.

[6] M. Kimiabeigi, and J. D. Widmer, "On winding design of a high performance ferrite motor for traction application," in *Proc. XXII Int. Conf. on Electrical Machines (ICEM)*, Lausanne, Switzerland, 4-7 Sept. 2016, pp. 1949-1956.

[7] L. Del Ferraro, and F.G. Capponi, "Aluminium multi-wire for high-frequency electric machines," in *Proc. 2007 IEEE Industry Applications Annual Meeting*, New Orleans, LA, USA, 23-27 Sept. 2007, pp. 89-93.

[8] K. Kovalev, J. Nekrasova, N. Ivanov, and S. Zhurzvlev, "Design of all-superconducting electrical motor for full electric aircraft," in *Proc. 2019 Int. Conf. on Electrotechnical Complexes and Systems (ICOECS)*, Ufa, Russia, 21-25 Oct. 2019, pp. 1-5.

[9] M. Iorgulescu, "Study of single phase induction motor with aluminium versus copper stator winding," in *Proc. 2016 Int. Conf. on Applied and Theoretical Electricity (ICATE)*, Craiova, Romania, 6-8 Oct. 2016, pp. 1-5.

[10] S. Ayat, R. Wrobel, J. Baker, and D. Drury, "A comparative study between aluminium and copper windings for a modular-wound IPM electric machine," in *Proc. 2017 IEEE Int. Electric Machines and Drives Conf. (IEMDC)*, Miami, FL, USA, 21-24 May 2017, pp. 1-8.

[11] H.I.H. Saravanamuttoo, G.F.C. Rogers, H. Cohen, P.V. Straznicky, and A. Nix, *Gas Turbine Theory*, 7th ed. Harlow: Pearson Prentice Hall, 2017.

[12] Anixter (2014). *Wire Wisdom: Copper vs Aluminium Conductors*. [Online]. Available: https://www.anixter.com/en_gb/resources/ literature/wire-wisdom/copper-vs-aluminum-conductors.html

[13] S.J. Salon, *Finite Element Analysis of Electrical Machines*. Boston: Kluwer Academic Publishers, 1995.

[14] K.J. Binns, P.J. Lawrenson, and C.W. Trowbridge, *The Analytical and Numerical Solution of Electric and Magnetic Fields*. Chichester: Wiley, 1992.

[15] J. Coulomb, and G. Meunier, "Finite element implementation of virtual work principle for magnetic or electric force and torque computation," *IEEE Trans. on Magnetics*, vol. 20, no. 5, pp. 1894-1896, Sept. 1984.

[16] D.M. Ionel, M. Popescu, M.I. McGilp, T.J.E. Miller, and S.J. Dellinger, "Assessment of torque components in brushless permanent-magnet machines through numerical analysis of the electromagnetic field," *IEEE Trans. on Industry Applications*, vol. 41, no. 5, pp. 1149-1158, Sept.-Oct. 2005.

[17] M. Popescu "Prediction of the electromagnetic torque in synchronous machines through Maxwell stress harmonic filter (HFT) method," *Electrical Engineering*, vol. 89, pp. 117-125, Dec. 2006.

[18] M. Popescu, D.M. Ionel, S. Dellinger, T.J.E. Miller, and M.I. McGilp, "Improved finite element computations of torque in brushless permanent magnet motors," IEE *Proc. Electrical Power Applications*, vol. 152, no.2, pp. 271-276, April 2005.

[19] T.J.E. Miller, M. Popescu, C. Cossar, and M.I. McGilp, "Performance estimation of interior permanent-magnet brushless motors using the voltage-driven flux-MMF diagram," IEEE *Trans. on Magnetics*, vol. 42, no. 7, pp. 1867-1873, July 2006.

[20] M. Rosu, P. Zhou, D. Lin, D. Lonol, M. Popescu, F. Blaabjerg, V. Rallabandi, and D. Staton, *Multiphysics Simulation by Design for Electrical Machines, Power Electronics and Drives*. Piscataway, NJ: IEEE Press; Hoboken, NJ: Wiley, 2018.